Evidence of Diffusion Regions at a Subsolar Magnetopause Crossing

F. S. Mozer, S. D. Bale, and T. D. Phan
Space Sciences Laboratory, University of California, Berkeley, California 94720
(Received 15 March 2002; published 12 June 2002)

On 1 April 2001, the Polar satellite crossed a subsolar magnetopause associated with antiparallel magnetic fields. Over a width ~6 magnetosheath ion skin depths (~3 magnetospheric ion skin depths), perpendicular ion flows different from $\mathbf{E} \times \mathbf{B}/B^2$ as well as Hall magnetic and electric field signatures were observed. At a smaller scale, the electron flow decoupled from the magnetic field near a deep minimum in the magnetic field strength. Separatrices were identified as boundaries of low frequency electric field turbulence associated with density minima and parallel electric fields. The reconnection rate was less than 2% of the asymptotic Alfvén speed.

DOI: 10.1103/PhysRevLett.89.015002 PACS numbers: 94.30.Di, 52.35.Vd, 52.70.Ds

Magnetic field reconnection is thought to control much of the topology and energetics of lab plasmas, the earth's magnetosphere, the sun, and all of astrophysics. Because it is best studied by *in situ* measurements in the earth's magnetosphere, considerable evidence has accumulated to show that magnetic field reconnection is responsible for modifying the topology of merging terrestrial and interplanetary magnetic fields to produce an open field line geometry that allows mass and momentum transfer from the solar wind into the magnetosphere. Magnetic field reconnection involves terms in the generalized Ohm's law that are ignored in magnetohydrodynamic (MHD) descriptions of the magnetosphere, which assume the "frozen-in" condition, $\mathbf{E} + \mathbf{v} \times \mathbf{B} = 0$, where $\mathbf{E}$ and $\mathbf{B}$ are the electric and magnetic fields, and $\mathbf{v}$ is the plasma bulk velocity. One such neglected term, producing the Hall effect, is the $\mathbf{j} \times \mathbf{B}$ force due to the current $\mathbf{j}$, whose inclusion causes decoupling of ions from the magnetic field at the ion skin depth to produce the ion diffusion region, quadrupolar magnetic fields [1–5], and bipolar electric fields [5,6]. On the smaller spatial scale of the electron diffusion region, electron inertial and gradient effects may become important to produce a parallel electric field, electrons that are decoupled from the magnetic field, and conversion of electromagnetic energy to particle energy [2,3,5] (see Fig. 1). Experimentally, direct encounters with the diffusion regions have been rare and details of these regions have not been well resolved. Partial confirmations of the ion-scale Hall effect have been reported as detection of the Hall magnetic field [7–9] and electron beams directed toward the separator along the separatrices [8–10]. Evidence for parallel electric fields and associated electron pressure effects has been reported in a complex crossing of a high latitude reconnection region [11] and in the auroral acceleration region [12,13]. The purpose of this Letter is to present a textbook example of a magnetopause crossing, where data from the only three-axis electric field experiment that has been flown in the outer magnetosphere [14] are combined with plasma and magnetic field measurements [15,16] to obtain an improved description of the ion and electron diffusion regions. Uncertainties in the electric and magnetic field measurements and the plasma data have been discussed elsewhere [11,17]. The basic reconnection configuration, the coordinate system, and observed features are described in Fig. 1.

The data of Figs. 2b through 2h have been rotated and transformed into a frame fixed to the magnetopause, with the X direction normal to the magnetopause surface, and with the plasma flowing from the magnetosheath in the $-X$ direction. This figure displays the crossing from the denser plasma (~5 cm^{-3} in Fig. 2a) and southward pointing magnetic field ($B_Z \sim -80$ nT in Fig. 2e) in the magnetosheath to the lower-density plasma (~1.5 cm^{-3}) and northward pointing field ($B_Z \sim 80$ nT) in the magnetosphere. Within the magnetopause, the magnetic field decreased to essentially zero within experimental uncertainties (Fig. 2b) while E_X (Fig. 2f) and B_Y (Fig. 2d) showed the expected signatures of Hall MHD in the ion diffusion region, where

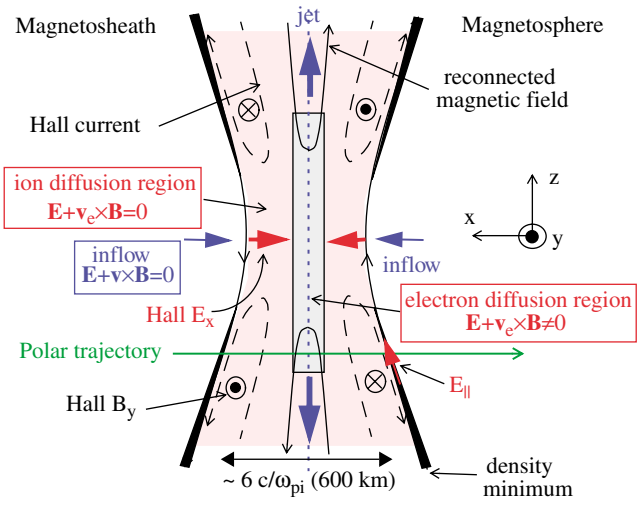

FIG. 1 (color). The geometry of the reconnection region with the results of the present experiment included. Note the coordinate description with X along the normal to the magnetopause. Ions are decoupled from the electrons and magnetic field in the ion diffusion region, creating the Hall magnetic and electric field patterns. Electrons are demagnetized in the electron diffusion region.

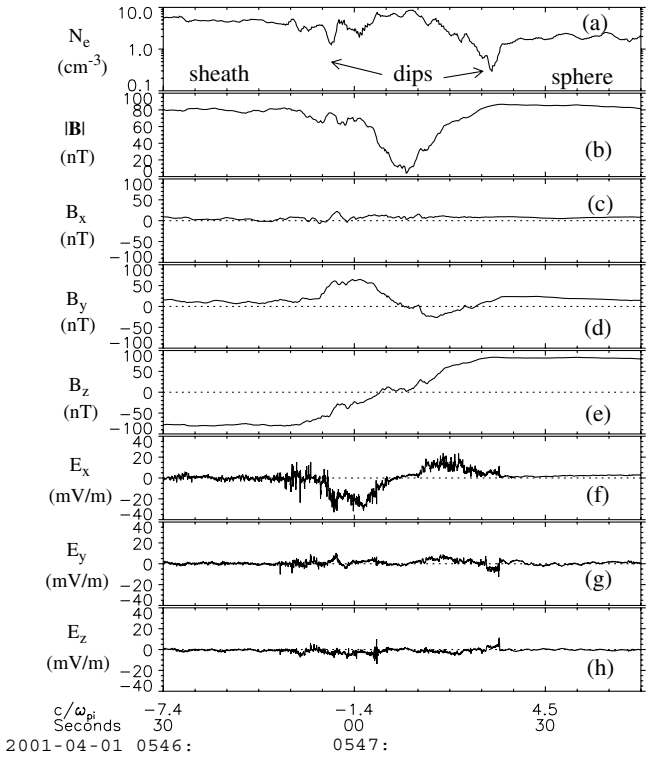

FIG. 2. Field and plasma data collected on 1 April 2001 at a geocentric altitude of 9.36 earth radii, a magnetic local time of 1145, and a magnetic latitude of 5.8°. Panel (a) is the plasma density determined from the 5 Hz spacecraft potential measurement normalized by the 0.6 Hz plasma density observations. The uncertainty in the density estimate is ~15% [20]. Panels (b), (c), (d), and (e) give, respectively, the magnitude and three components of the measured magnetic field at a rate of 8 samples/sec. Panels (f), (g), and (h) give the three components of the electric field in a frame fixed to the magnetopause and in which the magnetosheath plasma is incident in a direction normal to the magnetopause surface. The electric field data rate was 40 samples/sec. The electric field was obtained after notch filtering the on-axis component to remove a small spin tone, subtracting a dc offset from the on-axis measurement, and notch filtering the higher harmonics of the spin frequency in the spin plane measurements. Similar corrections were applied to the magnetic field data. The X direction of the GSE coordinate system of the original data points from the earth towards the sun, the Y direction lies in the ecliptic plane and points towards dusk, and Z is parallel to the ecliptic pole.

the ions did not obey $\mathbf{E} + \mathbf{v_i} \times \mathbf{B} = 0$. The normal magnetic field was ~5 nT (Fig. 2c). The entire magnetopause crossing took 28 sec.

Rotation from the spacecraft frame into boundary normal coordinates was accomplished in three different ways; through the maximum variance of the electric field, the minimum variance of the magnetic field, and from the Faraday residue method [18]. These three methods gave the same normal direction to within 11°. The GSE (defined in the caption of Fig. 2) minimum variance normal, $\mathbf{n} = (0.9613, 0.0538, 0.2703)$, was used for the coordinate rotation in Fig. 2. The plasma velocity and the electric field were next transformed into a frame moving in the X direction and fixed to the magnetopause by requiring that the tangential component of the electric field be continuous in the magnetopause frame. Finally, they were transformed into a frame that moved along the magnetopause surface and in which the magnetosheath plasma flow was incident on the magnetopause in the $-X$ direction.

Transformation from the spacecraft frame to a frame fixed to the magnetopause was accomplished by assuming that the static magnetopause had a constant tangential electric field as it moved in the X direction at a constant speed. The assumption of a constant speed is consistent with the smooth variation of B_Z in Fig. 2e. Given the fields $E_Y(1)$, $B_Z(1)$, $E_Y(2)$, and $B_Z(2)$ in the spacecraft frame at times 1 and 2, the requirement that the tangential electric field in the magnetopause frame be the same at these two times is that v_X, the speed of the magnetopause with respect to the spacecraft frame, be

$$v_X = [E_Y(1) - E_Y(2)]/[B_Z(1) - B_Z(2)]. \quad (1)$$

It is noted that this speed is insensitive to offset errors in the field measurements because it results from differences of such measurements. The data of Table I allow computation of an average v_X.

Early in Table I, the spacecraft was in the magnetosheath and E_Y and $(\mathbf{E} \times \mathbf{B}/B^2)_X$ were small. After about 24 sec, E_Y grew to a typical value of about -1.5 mV/m. The measured electric field was a remote sensor of magnetopause motion as the local plasma moved with the $(\mathbf{E} \times \mathbf{B}/B^2)$ velocity in response to the magnetopause beginning to move sunward, toward the spacecraft [19]. About 24 sec later, the magnetopause was entered, and the spacecraft entered the magnetosphere about 48 sec later. The magnetopause continued to move sunward for about a minute, at which time the electric field became large and negative, signifying that the magnetopause turned and

TABLE I. Twelve second averages of E_Y and B_Z through the magnetosheath, magnetopause (MP), and magnetosphere.

Seconds after 0546	E_Y mV/m	B_Z nT	Region
0–12	−0.3	−79.1	Sheath
12–24	−0.9	−78.8	Sheath
24–36	**−1.5**	**−78.9**	Sheath
36–48	**−1.8**	**−78.6**	Sheath
48–60	**−1.0**	**−59.4**	MP
60–72	1.0	2.2	MP
72–84	2.7	68.8	MP
84–96	1.4	82.4	Sphere
96–108	2.4	81.1	Sphere
108–120	2.3	78.7	Sphere
120–132	1.5	77.1	Sphere
132–144	1.2	75.4	Sphere
144–156	1.6	72.4	Sphere
156–168	−0.6	71.6	Sphere
168–180	−4.5	71.9	Sphere

was returning toward the spacecraft. Indeed, a second magnetopause crossing did occur 3 min following the data in Table I.

The average magnetopause speed, as computed from Eq. (1), using 25 combinations of Table I data, was 23.7 ± 4.9 km/sec. These 25 combinations include each of the bold data points in the table (the magnetosheath data) with every one of the following points other than the last two, by which time the magnetopause speed had changed. Two of the 27 combinations thus produced were discarded for being more than two standard deviations from the mean. The Faraday residue method [18], which generates a slightly different magnetopause normal, yielded a similar speed of 20.6 km/sec. From the average of these velocities, time, at the bottom of Fig. 2, has been converted to distance in units of the magnetosheath ion skin depth, $c/\omega_{\rm pi} = 100$ km, where $\omega_{\rm pi}$ is the ion plasma frequency. The thickness of the magnetopause was about 6 magnetosheath ion skin depths (or ~3 magnetospheric ion skin depths) at the crossing location of the Polar satellite.

The velocity along the magnetopause surface required to transform from the magnetopause frame to the frame in which the magnetosheath plasma was incident in the $-X$ direction is $(0, 9 \pm 36, 60 \pm 22)$ km/sec, and the tangential electric field in this new frame is 0.4 mV/m. The uncertainty of this field estimate is ~2 mV/m.

Figure 3 compares the components of the perpendicular ion and electron flows with the components of ($\mathbf{E} \times \mathbf{B}/B^2$). In Fig. 3c, the ion flow (the dashed horizontal lines) differed significantly from $(\mathbf{E} \times \mathbf{B}/B^2)_Z$ (the black points) throughout the magnetopause. This is another manifestation, along with the bipolar signatures in $\mathbf{E}$ and $\mathbf{B}$, that the spacecraft was in the ion diffusion region where $\mathbf{E} + \mathbf{v_i} \times \mathbf{B} \neq 0$ through the passage. The predominately negative values of the electron flow (the solid horizontal lines) and of $(\mathbf{E} \times \mathbf{B}/B^2)_Z$ signify that the spacecraft crossed the magnetopause south of the separator, in agreement with the signs of the bipolar magnetic field signature and the outward pointing normal magnetic field. The maxima of the perpendicular electron flow speed and $(\mathbf{E} \times \mathbf{B}/B^2)_Z$ were about 60% of the magnetosheath Alfvén speed of 700 km/sec, while the perpendicular ion speed did not exceed 20% of this Alfvén speed.

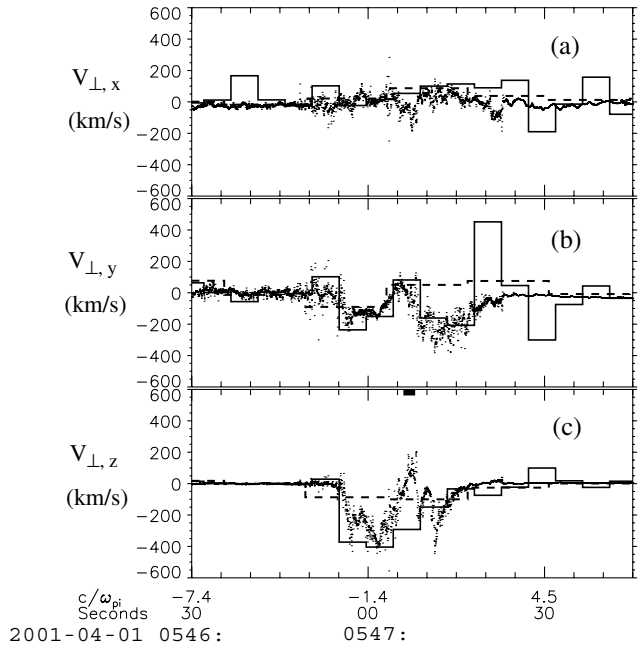

FIG. 3. Components of the ion and electron perpendicular flows and $\mathbf{E} \times \mathbf{B}/B^2$ in the normal incidence frame. The solid and dashed lines result from averaging the first moments of the electron and ion distributions over the illustrated time intervals. $\mathbf{E} \times \mathbf{B}/B^2$ is computed 40 times/sec from the instantaneous electric field measurements and the interpolated 8 Hz magnetic field data.

The Z component of the perpendicular electron flow in Fig. 3c differed from $(\mathbf{E} \times \mathbf{B}/B^2)_Z$ for about 2 sec near 0547:07 (the interval marked by a thick horizontal bar in Fig. 3c), when the electron flow was about −300 km/sec while $(\mathbf{E} \times \mathbf{B}/B^2)_Z$ changed sign and became as large as +150 km/sec. The standard deviation of the electron perpendicular flow is estimated to be ≈75 km/sec at this time [20], as is the uncertainty of $(\mathbf{E} \times \mathbf{B}/B^2)_Z$ in this small field region. The uncertainty estimates are consistent with the spread in the flow data at other times, particularly in the magnetosphere where the lower density and higher temperature combine to increase the uncertainty in the electron flow. The several-standard-deviation difference between $(\mathbf{E} \times \mathbf{B}/B^2)_Z$ and the perpendicular electron flow near 0547:07 suggests the decoupling of electron motion from the magnetic field that is expected in the electron diffusion region, within which $\mathbf{E} + \mathbf{v_e} \times \mathbf{B} \neq 0$, where $\mathbf{v_e}$ is the electron flow velocity. The 2 sec width of this region is about 0.4 magnetosheath ion skin depths or 15 magnetosheath electron skin depths. It is noted that the horizontal bar representing the electron flow between about 0547:04.3 and 0547:08.9 results from two 1.15 sec measurements that start at 0547:05.4 and 0547:07.7 and that are made simultaneously in 12 electron detectors.

The separatrices that bound the magnetopause are associated with local minima in the plasma density of Fig. 2a, boundaries in the low frequency electric field turbulence of Figs. 2f–2h, and achievement by the magnetic field components of their asymptotic values in Figs. 2d and 2e. There is also a parallel electric field associated with the magnetospheric separatrix, as illustrated in Fig. 4, in which panels 4a and 4b give the plasma density and the parallel electric field, respectively. During this 5 sec interval, the magnetic field was nearly in the spacecraft spin plane such that the relatively larger uncertainties of the spin axis electric field measurement did not affect the parallel field data. It is noted that the largest parallel electric fields were measured in the vicinity of the largest changes in the plasma density, in accordance with the expectation from the generalized Ohm's law that such parallel fields are supported by the divergence of the pressure tensor.

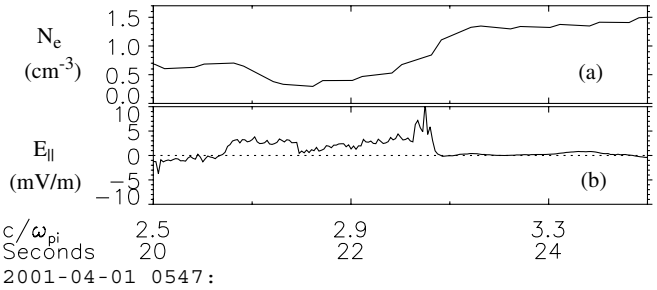

FIG. 4. Plasma density and the parallel electric field at the crossing of the magnetospheric separatrix.

These observations can be summarized and interpreted as follows:

1. Hall MHD and the ion diffusion region: Signatures of Hall MHD and the ion diffusion region (the lightly tinted region in Fig. 1) were seen in the Y component of the magnetic field (the arrows into and out of the paper in Fig. 1), the X component of the electric field (the red horizontal arrows), and the disagreement between the perpendicular ion flow and $(\mathbf{E} \times \mathbf{B}/B^2)_Z$. The amplitude of the Hall B_Y was ~45 nT, or $\sim 0.55 B_0$, where B_0 is the asymptotic magnetic field in the magnetosheath. This compares with the simulation result of $\sim 0.35 B_0$ [2,21]. The maximum normal electric field was ~30 mV/m or $\sim 0.5 v_{\text{Alfvén}} B_0$, which is equal to the simulation result [21]. The ion diffusion region had a width of about 6 magnetosheath ion skin depths (or ~3 magnetospheric ion skin depths) at the location of the spacecraft crossing.

2. The electron diffusion region: Partial evidence for the electron diffusion region (the gray tinted region in Fig. 1) was seen in the decoupling of the electron flow from $(\mathbf{E} \times \mathbf{B}/B^2)_Z$ during a 2 sec interval and a deep minimum in the magnetic field. The width of this region was ~15 magnetosheath electron skin depths (or ~8 magnetospheric electron skin depths). The reversal of $(\mathbf{E} \times \mathbf{B}/B^2)_Z$ in this central region has not been predicted.

3. The tangential electric field: The tangential electric field at the magnetopause was smaller than the measurement uncertainty of about 2 mV/m, which corresponds to an inflow rate $< 0.02 v_{\text{Alfvén}}$. This rate is an order-of-magnitude smaller than that expected from some computer simulations [2,3,15] but it agrees with others [22].

4. The normal magnetic field: The magnetic field component normal to the magnetopause layer was 5 nT. Because of its near constancy with time, it is a robust estimate that does not depend on the interval over which it is estimated.

5. The spacecraft location: The spacecraft crossed the magnetopause south of the separator (the green trajectory in Fig. 1). That the crossing was not far from the separator is evidenced by the fact that the plasma flows were sub-Alfvénic. The maximum ion flow speed was about 300 km/sec or $\sim 0.4 v_{\text{Alfvén}}$, and the maximum electron flow speed was about 500 km/sec or $\sim 0.7 v_{\text{Alfvén}}$. Evidence that the crossing was south of the separator comes from $(\mathbf{E} \times \mathbf{B}/B^2)_Z$ being negative, B_X being positive, and the sign of the bipolar Hall B_Y being that expected for a southward crossing.

6. The observation of separatrices: The separatrix on the magnetospheric side of the magnetopause was well measured as a boundary between turbulent and quiet electric fields that contained a minimum in the plasma density (the thick black lines in Fig. 1) [3], a parallel electric field (the red arrow along the separatrix in Fig. 1), and a magnetic field that reached its asymptotic value. The data also indicate the crossing of the separatrix on the magnetosheath side of the magnetopause.

The authors thank C. Russell and J. D. Scudder for use of data from the magnetometer and plasma experiments on Polar. We also thank M. Fujimoto, Y. Lin, J. D. Scudder, M. Shay, and B. Sonnerup for valuable discussions. This research was supported by NASA Grants No. NAG5-8078 and No. NAG5-7883.

[1] B. U. Ö. Sunnerup, in *Solar System Physics,* edited by L. T. Lanzerotti, C. F. Kennel, and E. N. Parker (North-Holland, New York, 1979), Vol. III, pp. 45–108.
[2] M. Hesse *et al.,* J. Geophys. Res. **106,** 3721 (2001).
[3] M. A. Shay *et al.,* J. Geophys. Res. **106,** 3759 (2001).
[4] Z. W. Ma and A. Bhattacharjee, J. Geophys. Res. **106,** 3773 (2001).
[5] P. L. Pritchett, J. Geophys. Res. **106,** 3783 (2001).
[6] M. A. Shay *et al.,* J. Geophys. Res. **103,** 9165 (1998).
[7] X. H. Deng *et al.,* Nature (London) **410,** 557 (2001).
[8] M. Oieroset *et al.,* Nature (London) **412,** 414 (2001).
[9] T. Nagai *et al.,* J. Geophys. Res. **106,** 25 929 (2001).
[10] M. Fujimoto *et al.,* Geophys. Res. Lett. **24,** 2893 (1997).
[11] J. D. Scudder *et al.,* J. Geophys. Res. (to be published).
[12] F. S. Mozer and A. Hull, J. Geophys. Res. **106,** 5763 (2001).
[13] R. E. Ergun *et al.,* Phys. Rev. Lett. **87,** 045003 (2001).
[14] P. R. Harvey *et al.,* Space Sci. Rev. **71,** 583 (1995).
[15] C. T. Russell *et al.,* Space Sci. Rev. **71,** 563 (1995).
[16] J. D. Scudder *et al.,* Space Sci. Rev. **71,** 459 (1995).
[17] F. S. Mozer and C. A. Kletzing, Geophys. Res. Lett. **25,** 1629 (1998).
[18] A. V. Khrabrov and B. U. Ö. Sonnerup, Geophys. Res. Lett. **25,** 2373 (1998).
[19] G. Paschmann *et al.,* Geophys. Res. Lett. **17,** 1829 (1990).
[20] J. D. Scudder (private communication).
[21] P. L. Pritchett, J. Geophys. Res. **106,** 25 929 (2001).
[22] X. Wang *et al.,* J. Geophys. Res. **105,** 27 633 (2000).